

A Study on the Corrosion Behavior of 15CrMo in Steam-Injection Boiler with Low-quality Feed Water

Jun Chen¹, Bing Bai², Naifeng Zhang¹, Gang Xiao¹, Yue Zhang¹, Lei Deng², Defu Che^{2*}

1 Steam Injection Technical Service Center, Shengli Oilfield, Sinopec, Dongying, 257001, China

2 State Key Laboratory of Multiphase Flow in Power Engineering, School of Energy and Power Engineering, Xi'an Jiaotong University, Xi'an, 710049, China

ABSTRACT

To obtain the corrosion behavior of a widely-used boiler steel (15CrMo) exposing to saline gas and saline water with sodium sulfate (Na_2SO_4), the experiments were designed and implemented. The samples were analyzed by scanning electron microscopy/energy disperse spectrum (SEM/EDS) and X-ray diffraction (XRD). The results show the different corrosion behavior between liquid phase and gas phase. The particles among corrosion products in gas phase are larger than that in liquid phase corrosion. The crystal structures of Fe_3O_4 could fully form in gas phase. The corrosion products in liquid phase are complicated, including Fe, Fe_2O_3 , Fe_3O_4 . The corrosion behavior of 15CrMo in saline circumstances could deeply influence the efficiency and safety of the boilers.

Keywords: Steam-injection boiler; Corrosion; Saline circumstances; 15CrMo steel

NONMENCLATURE

Symbols	
V_l	volume of liquid phase(m^3)
V_g	volume of gas phase(m^3)
ρ_l	density of liquid phase (kg m^{-3})
ρ_g	density of gas phase (kg m^{-3})

1. INTRODUCTION

The safety and efficiency of boilers could be significantly influenced by the corrosion behavior of the employed steels [1-3]. Pipe broken accidents in boilers have triggered off many severe economic and safety problems caused by corrosion. Some studies [4-10] have been conducted to figure out the corrosion behaviors of boiler tubes. These researches could be classified into fireside corrosion and working medium side corrosion. For instance, Xiong *et al.* [10] investigated the high-temperature corrosion behavior of water cooled wall tubes on the fireside at a 300 MW boiler. Wang *et al.* [4] conducted an experimental study on dew point corrosion characteristics of the heating surface on the fireside in a biomass-fired boiler. Xu *et al.* [11] investigated the effect of pre-oxidation on the steam oxidation of T92 heat-resistant steel at 650 °C. Ishitsuka *et al.* [12] conducted a study on the steam corrosion behavior of 9Cr-0.5Mo-1.8W steel at high temperatures.

Meanwhile, the corrosion behavior is tightly related to the quality of feed water. In power plant, feed water is well treated so that impurities could be reasonably ignored [9, 13]. Steam-injection boilers are widely used in oil recovery and extraction of bitumen. During the operation of steam-injection boilers, large volumes of water and steam are injected into the oil well without reusing [14, 15]. Thus, the consumption of water in steam-injection boilers is larger than many other boilers, which leads to the limitation of the water treatment budget. Therefore, salinity could change the corrosion behavior of boiler steel [16].

The results of water quality detection in Shengli oilfield indicate that sodium sulfate is one of the most

abundant salt in the feed water of the steam injection boiler. The boiler steel is made of 15CrMo. Therefore, the study focused on the corrosion behavior of 15CrMo steel in saline (sodium sulfate) circumstances.

2. EXPERIMENTAL DETAILS

2.1 Sample preparation

Table 1 Chemical composition of studied material 15CrMo steel (wt. %-mass fraction)

Element	C	Si	Mn	S	P	Cr	Mo	Fe
wt. %	0.15	0.15-0.40	0.40-0.70	0.03	0.03	0.80-1.20	0.45-0.60	Balance

2.2 Experimental apparatus

The autoclave employed in our experiments is capable of withstanding high temperature and high pressure, which could be up to 370 °C and 25 MPa, respectively. The figure of the autoclave is shown in Fig.1.

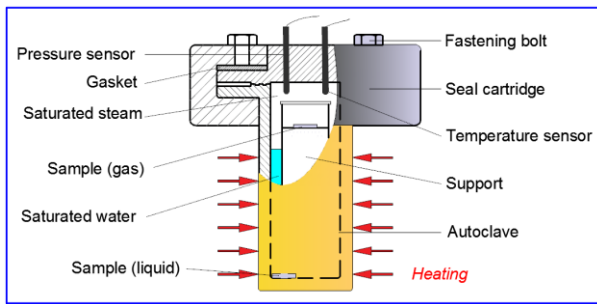


Fig.1 Experimental apparatus

The mass of solution added into the autoclave must be limited in a certain range. On the one hand, when the temperature inside the autoclave stabilized at a set value, liquid and gas must coexist to maintain the saturated condition. On the other hand, the sample in gas phase is prohibited to be exposed to liquid. Therefore, the mass is controlled by the following equations,

$$\begin{cases} V_l / S < h \\ \rho_l V_l + \rho_g V_g = m \\ V_l + V_g = V \\ m > \rho_g V \end{cases} \quad (1)$$

Where V_l and V_g are the volumes of liquid phase and gas phase at the specific condition, S is the basal area of the autoclave, h represents the height of the top place where the sample is positioned, ρ_l and ρ_g are the densities of liquid phase, and gas phase at the specific

The 15CrMo flakes are used as tested samples in the autoclave. The treated samples are put into the autoclave for corrosion experiments. The inner wall of the autoclave is made of Hastelloy C276. It is chemically stable under experimental conditions. Its good properties make it possible to keep samples from pollution as far as possible. The chemical composition of 15CrMo is presented in Table 1.

condition respectively. V is the volume of autoclave. m is the mass of solution added into the autoclave.

The expression of solution mass could be derived from Eq. (1) as,

$$\rho_g V < m < hS(\rho_l - \rho_g) + \rho_g V \quad (2)$$

Therefore, the mass of the solution could be determined by Eq. (2).

3. RESULT AND DISCUSSION

3.1 The corrosion of boiler steel in liquid phase

To study the corrosion behavior of 15CrMo steel in saline liquid, the detection on the corroded surface is implemented, including XRD and SEM/EDS analysis. The XRD result has been shown in Fig.2. The heating temperature in the autoclave (T) is 350 °C. The heating time (t) is 300 h.

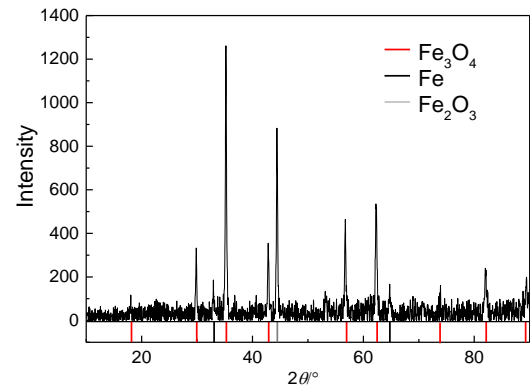


Fig.2 The XRD result of the corroded surface (liquid phase)

As shown in Fig.2, there are peaks corresponding to three kinds of crystal products detected. The corresponding substances are Fe, Fe₂O₃ and Fe₃O₄ respectively. Among all the peaks, the number of Fe₃O₄ is more than those of Fe and Fe₂O₃ as the number of

peaks corresponding to Fe_3O_4 is larger. It demonstrated that the crystal structures of Fe_3O_4 are fully generated during the corrosion process in the liquid phase. Therefore, the experimental condition is suitable for the formation process of Fe_3O_4 . Besides, the SEM and EDS analysis are also implemented. The results are shown in Table 2, Fig. 3 and Fig. 4.

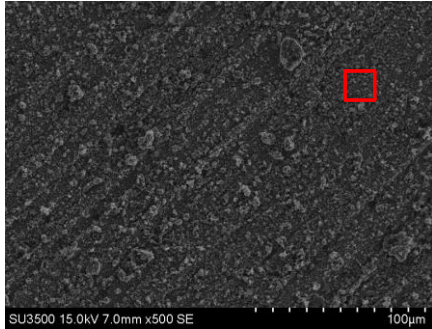


Fig. 3 SEM image of corroded surface (liquid phase)

Table 2 EDS analysis of the corroded sample (liquid phase)

Element	C	O	Fe
wt. %	4.02	24.25	71.73

As could be seen in Fig. 3, the corroded surface is covered by small particles equably. These small particles come from the oxidation and corrosion. The EDS results indicate that the main elements are C, O and Fe, among which the mass fraction of Fe is up to 71.73%. Carbon comes from the steelmaking process. The results indicate that the main corrosion product are Fe_3O_4 as the morphologies of corroded surface is basically unique. The XRD analysis demonstrates the well-generated structure of Fe_3O_4 .

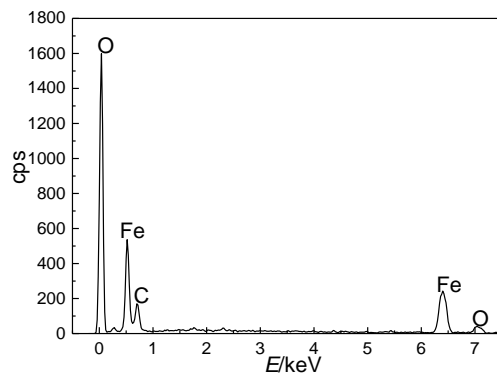


Fig. 4 The EDS result of the corroded surface (liquid phase)

3.2 The corrosion of boiler steel in gas phase

In this part, the corrosion behavior of 15CrMo steel in gas phase is studied. The heating temperature in the autoclave (T) is 350 °C. The heating time (t) is 300 h. The experimental condition is consistent with that in gas-

phase corrosion. The SEM image of the corroded surface is shown in Fig. 5. The corresponding EDS analysis is shown in Table 3 and Fig. 6.

It could be seen in Fig. 5 that the particles are larger than that in Fig. 3 on the same scale ($\times 500$) under the microscope.

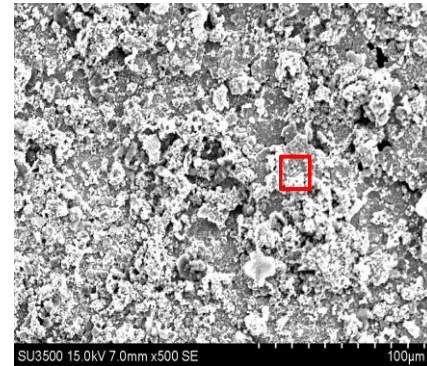


Fig. 5 SEM image of corroded surface (gas phase)

Besides, the spectrum of EDS analysis presents the peaks of each element. As could be seen in Table 3, the main elements detected on the surface by EDS are Cr, O and Fe. Compared with the result in liquid phase, the mass fractions of Fe and O are basically the same, respectively. The morphologies are also different. In Fig. 5, the size of particles cluster in irregular shapes is larger than that in Fig. 3. It indicates a higher level of the accumulation among corrosion products.

Table 3 EDS analysis of the corroded sample (gas phase)

Element	Cr	O	Fe
wt. %	9.79	22.01	68.21

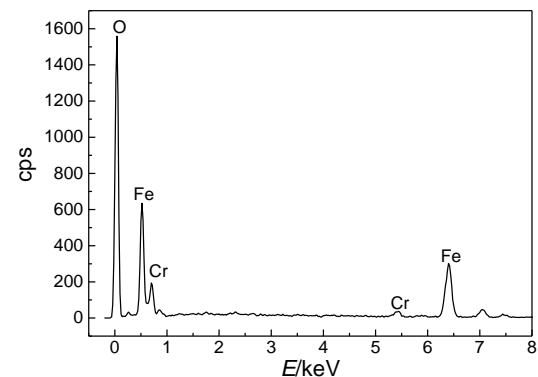


Fig. 6 The EDS result of the corroded surface (gas phase)

Fig. 7 shows the XRD analysis of the corroded surface in the gas phase. The results indicate that all the main peaks detected in the spectrum correspond to the crystal structures of Fe_3O_4 . Fe_3O_4 is fully generated in gas phase. Compared with the corrosion behavior in the liquid phase, Fe and other Fe oxides except Fe_3O_4 in crystal structure does not exist anymore. Therefore, the gas

phase circumstances could promote the formation of Fe_3O_4 .

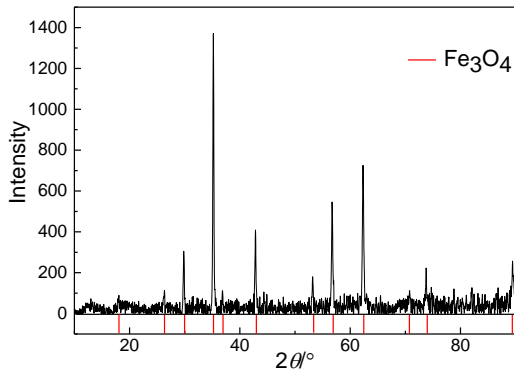


Fig.7 The XRD result of the corroded surface (gas phase)

4. CONCLUSION

Exposing to saline liquid and saline gas phase, the corrosion behavior of 15CrMo steel, which is widely used in the boiler tube manufacturing, are studied in this paper. In the gas-phase corrosion, the crystal structure of Fe_3O_4 could fully form on the corroded surface. The corrosion products fully are accumulated in the gas phase. Meanwhile, in the liquid phase, the particles on the corroded surface is relatively smaller than that in the gas phase. Besides, the substances detected are composed of Fe, Fe_2O_3 and Fe_3O_4 . In this point of view, when the temperature and pressure are fixed, the corrosion process in the gas phase is more severe than that in the liquid phase.

REFERENCE

- [1] Jelovica I, Kavre I, Peter R, Saric I, Petravic M. Formation of oxides on CoCrMo surfaces at room temperature: An XPS study. *Appl Surf Sci.* 2019;471:475-481.
- [2] Taurino A, Forleo A, Francioso L, Siciliano P, Stalder M, Nesper R. Synthesis, electrical characterization, and gas sensing properties of molybdenum oxide nanorods. *Appl Phys Lett.* 2006;88:152111.
- [3] Qi W, Chen S, Wu Y, Xie K. A chromium oxide coated nickel/yttria stabilized zirconia electrode with a heterojunction interface for use in electrochemical methane reforming. *RSC Adv.* 2015;5:47599-47608.
- [4] Wang Y, Ma H, Liang Z, Chen H, Jin, X. Experimental study on dew point corrosion characteristics of the heating surface in a 65 t/h biomass-fired circulating fluidized bed boiler. *Appl Therm Eng.* 2015; 96:76-82.
- [5] Bang J, Kim Y, Kim S, Shin D, Cho K, Kwon W. High Temperature Corrosion Properties of Heating Surface in Waste-to-Energy Boiler Tube. *Journal of Korea Society of Waste Management.* 2017;34: 27-33.
- [6] Li Z, Sun F, Shi Y, Li F, Ma L. Experimental study and mechanism analysis on low temperature corrosion of coal fired boiler heating surface. *Appl Therm Eng.* 2015;80: 355-361.
- [7] Kaushal G, Singh H, Prakash S. Surface engineering, by detonation-gun spray coating, of 347H boiler steel to enhance its high temperature corrosion resistance, *Mater High Temp.* 2014;28:1-11.
- [8] Xu L, Huang Y, Wang J, Liu C, Liu L, Zou L, Yue J, Chen K. Experimental investigation of high-temperature corrosion properties in simulated reducing-sulphidizing atmospheres of the waterwall fireside in the boiler. *The Canadian Journal of Chemical Engineering.* 2020;98.
- [9] Kumar M, Joshna K, Markendeya R, Rawat M. Effect of steamside oxidation and fireside corrosion degradation processes on creep life of service exposed boiler tubes. *Int J Pres Ves Pip.* 2016;144.
- [10] Xiong X, Liu X, Tan H, Deng S. Investigation on high temperature corrosion of water-cooled wall tubes at a 300 MW boiler. *J Energy Inst.* 2020;93.
- [11] Xu H, Liang Z, Ding J, Zhao Q, Guan S. Effect of Pre-Oxidation on the Steam Oxidation of Heat-Resistant Steel T92. *High Temp Mat Pr-Isr.* 2018; 37:733-739.
- [12] Ishitsuka T, Inoue Y, Ogawa H. Effect of Silicon on the Steam Oxidation Resistance of a 9%Cr Heat Resistant Steel. *Oxid Met.* 2004; 61:125-142
- [13] Deodeshmukh V, Pint B. Fireside Corrosion and Steamside Oxidation Behavior of HAYNES 282 Alloy for A-USC Applications. *Asm International, Materials Park.* 2016.
- [14] Lu J, Wang X, Shan B, Li X, Wang W. Analysis of chemical compositions contributable to chemical oxygen demand (COD) of oilfield produced water. *Chemosphere.* 2006;62: 322-331.
- [15] Dong B, Ying X, Jiang S, Dai X. Effect of reusing the advanced-softened, silica-rich, oilfield-produced water (ASOW) on finned tubes in steam-injection boiler. *Desalination.* 2015;372: 17-25.
- [16] Onyeachu B, Oguzie E, Ukaga I, Njoku D, Peng X. Ni Corrosion Product Layer During Immersion in a 3.5% NaCl Solution: Electrochemical and XPS Characterization. *Portugaliae Electrochimica Acta.* 2017; 35:127-136.